Mikada, H., Moore, G.F., Taira, A., Becker, K., Moore, J.C., and Klaus, A. (Eds.)
Proceedings of the Ocean Drilling Program, Scientific Results Volume 190/196

16. Data Report: Reprocessing of Wireline Sonic Logs in Turbidites and Hemipelagic Sediments at ODP Site 1173[1]

David Goldberg[2]

ABSTRACT

High-quality sonic log waveforms were recorded during Leg 190 from 65- to 360 m below seafloor (mbsf) in Hole 1173A. Schlumberger's wireline Dipole Shear Imager (DSI) tool was used, and the data were reprocessed using a phase-picking method to improve the shipboard *P*- and *S*-wave logs. This postcruise work focused on evaluating the high variability observed in the *P*-wave log in the upper interval of the hole and an inversion (low V_P and V_S) below 350 mbsf. In these intervals, sonic signals were weak and difficult to identify using standard shipboard processing methods. The outcome of the reprocessing was successful and extracted improved *P*-wave logs and *S*-wave values as low as 280 m/s in the upper interval of the hole and below 350 mbsf. The reprocessed data are currently available online at **www.ldeo.columbia.edu/BRG/ODP/DATABASE/index.html.**

INTRODUCTION AND BACKGROUND

Leg 190 drilling on the Nankai Trough accretionary prism was the first of a two-leg program concentrating on coring and sampling a transect of sites across the prism within a three-dimensional (3-D) seismic survey. Previous drilling in this area, however, provides relatively little constraint on seismic velocities (also see Moore et al., 2001). During Ocean Drilling Program (ODP) Leg 190, six sites along two transects across the Nankai Trough accretionary prism were successfully drilled.

[1]Goldberg, D., 2003. Data report: Reprocessing of wireline sonic logs in turbidites and hemipelagic sediments at ODP Site 1173. *In* Mikada, H., Moore, G.F., Taira, A., Becker, K., Moore, J.C., and Klaus, A. (Eds.), *Proc. ODP, Sci. Results,* 190/196, 1–15 [Online]. Available from World Wide Web: <http://www-odp.tamu.edu/publications/190196SR/VOLUME/CHAPTERS/209.PDF>. [Cited YYYY-MM-DD]
[2]Lamont-Doherty Earth Observatory, Borehole Research Group, PO Box 1000, 61 Route 9W, Palisades NY 10964, USA.
goldberg@ldeo.columbia.edu

Initial receipt: 17 November 2002
Acceptance: 15 May 2003
Web publication: 25 July 2003
Ms 190SR-209

Only one reference site (Site 1173) at the seaward end of the Muroto Transect was logged using the ODP wireline tool strings (Shipboard Scientific Party, 2000). Leg 196 used logging-while-drilling (LWD) technology to collect additional in situ physical properties data from Site 1173 as well as from Site 808 along the Muroto Transect (Shipboard Scientific Party, 2001c). The wireline and LWD data sets are complementary; when combined, they can provide accurate constraints on the in situ physical properties.

Sonic logs provide one of the best means to investigate the acoustic properties of a formation as a continuous function of depth and to tie logging data with seismic and core measurements (e.g., Goldberg, 1997). During Leg 190, the Schlumberger Dipole Shear Sonic Imager (DSI) tool was used to record sonic logs (see Shipboard Scientific Party, 2001a). This tool utilizes a combination of monopole and dipole transducers in an array (Fig. **F1**) and is deployed typically in combination with other tools such as the Formation MicroScanner and natural gamma ray tools (**www.ldeo.columbia.edu/BRG/ODP/LOGGING/TOOLS/tool.shtml**). Dipole sonic tools such as the DSI are designed to excite both compressional and flexural energy in the borehole (Winbow, 1985) and are thus able to directly measure both *P*- and *S*-wave speeds in all type of formations so long as good borehole conditions persist. In unconsolidated formations, such as the turbidites and hemipelagic mud drilled at Site 1173, the flexural mode is excited by a low-frequency asymmetric source in the tool and travels at the *S*-wave velocity at its low-frequency cutoff (Winbow, 1985). This provides a reliable measure of the *S*-wave velocity where it would otherwise not be measurable.

F1. Schematic of the DSI tool, p. 8.

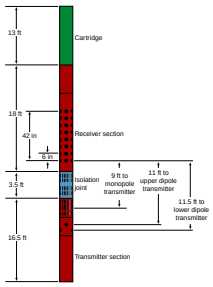

LOGGING OPERATIONS AND HOLE CONDITIONS

Logging operations in Hole 1173A are described in Shipboard Scientific Party (2001b). For this work, it is important to note that two passes of the DSI were made over the interval from 65 to 360 m below the seafloor (mbsf) through lithostratigraphic units composed of sandy to muddy turbidites, some volcanic ash, and silty and siliceous claystones (Shipboard Scientific Party, 2001d). The hole was drilled with a 9.875-in bit that was raised to a depth of 65 mbsf prior to logging. The logging tool was not able to reach the total drilled depth in Hole 1173A due to bridging of the hole at 380 mbsf, and efforts to clear this obstruction deteriorated the shallow hole conditions to some extent. Before logging, 50 bbl of sepiolite mud was pumped into the hole, and then, to further stabilize the hole, ~225 bbl of 10.5-ppg weighted barite mud was pumped in the hole to 637 mbsf (well below the first log reading). As a result, the borehole fluid properties and any change in fluid invasion into the formation are likely to be similar between the two passes. Both of the DSI passes were run at the same logging speed using the wireline heave compensator (Goldberg, 1990). Pass 1 recorded the high-frequency upper dipole plus *P*- and *S*-wave modes, and pass 2 recorded the low-frequency lower dipole plus *P*- and *S*-wave modes. The low-frequency (<1 kHz) dipole source was used for the second pass to enhance the flexural wave energy.

In Figure **F2,** the caliper log shows the hole diameter in orthogonal directions from both logging passes. Hole diameter is variable and enlarged from 100 to 220 mbsf along one axis and otherwise relatively constant to a depth of 360 mbsf. The measured shape of the borehole

F2. Caliper logs from the DSI tool, p. 9.

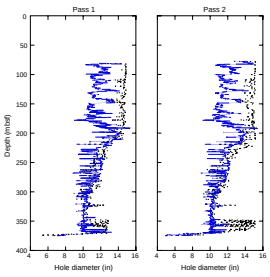

remains essentially unchanged between passes. Enlarged and rugose borehole conditions, such as those observed in the upper interval, degrade sonic logging data (e.g., Goldberg et al., 1984).

DSI DATA PROCESSING

Raw *P*- and *S*-wave data from the DSI were processed to extract *P*- and *S*-wave slowness (inverse of velocity) in Hole 1173A. A phase-picking algorithm is used, fully described by Kozak et al. (2001), that is based on the Hilbert transform of time domain signals and typically uses 16 points per cycle to identify the arrival times of various wave modes. Real-time picking and semblance processing algorithms are often used for computation of *P*- and *S*-wave logs by commercial logging services (e.g., Kimball and Marzetta, 1984), but caution is advised if high-resolution results are desired or when enlarged hole conditions are present. In these cases, resolution may be lost by averaging across the receiver array or from noisy and unstable receivers at certain depths. Using the high-resolution phase-picking method and selecting receivers for processing improves the slowness estimates significantly. In addition, frequency filtering, wave propagation modeling, stacking, and other numerical techniques are used prior to the slowness picking to achieve the highest quality results.

P-WAVE PROCESSING

In Figure **F3,** raw *P*- and *S*-wave data recorded at receivers 1 and 4 and frequency spectra for receiver 1 (*P*-wave) and for receiver 5 (*S*-wave) are shown. The spectral plot indicates that most of recorded *P*-wave energy exists in the 10- to 13-kHz and 16- to 18-kHz frequency bands. Modeling indicates that the *P*-wave signal (the earliest arriving energy) is negligible above about 10 kHz, and late-arriving high-energy fluid and borehole modes generate these peaks. In these soft sediments, especially in the shallow interval, the formation *P*-wave velocity approaches the fluid velocity and these modes mix. This causes artifacts in the shipboard log because the software "switches" between picking the *P*-wave and the high-energy fluid modes. With enlarged hole conditions, the fluid arrivals are stronger and mode switching increases, generating a variable and unreliable log.

To remove this effect, filters were applied on the raw monopole data over a fixed frequency range from 5500 to 8500 Hz to isolate the *P*-wave energy. This bandpass filter was run three times for pass 1 and once for pass 2. In addition, the *P*-wave arrives earliest in the wavetrain and was separated from other later-arriving modes, such as the direct fluid and Stoneley arrivals, by selecting a variable time window length of 1450–1600 ms starting at 1400 ms for pass 1 and 1900 ms for pass 2. Testing shows that these parameter differences between pass 1 and pass 2 produce a negligible change in the results. A fixed slowness range from 80 to 280 ms/ft was used, and *P*-wave slowness is determined automatically by picking the first arrival time in the filtered data for both passes. The *P*-wave mode is also nondispersive at these frequencies (Paillet and White, 1982), and no subsequent corrections are required. Sufficient energy and high signal-to-noise in these data enable results to be obtained over the entire interval for both logging passes. Differences between the two passes are discussed below.

F3. Wireline DSI data, p. 10.

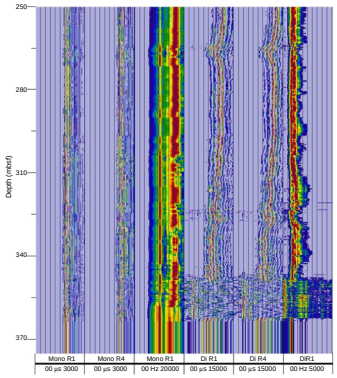

S-WAVE PROCESSING

Because of the low *S*-wave velocity in these formations (below the compressional velocity of the borehole fluid), *S*-wave information must be extracted from the flexural wave at its low-frequency cutoff (Winbow, 1985). The excitation of this mode depends on the *S*-wave slowness of the formation, the borehole size, and the resonant frequency of the flexural mode from the DSI tool. Modeling of the flexural mode poles under the conditions encountered at Site 1173 is shown in Figure F4. A strong resonant peak of the flexural mode at ~780 ms/ft occurs below 1000 Hz. Energy decreases at slowness values away from this peak and at frequencies above 2500 Hz. Other minor peaks occur at low slowness values and are due to scattered energy from the dipole source in the DSI tool. Thus, in order to eliminate the effect of resonant tool energy, the raw dipole waveforms were filtered over a frequency range from 250 to 750 Hz to extract the flexural mode only. This bandpass filter was run three times to reduce windowing edge effects.

The modeling of the flexural wave also shows that dispersion only occurs above ~500 Hz under these conditions. Correction of the flexural wave dispersion is therefore not required for these data (e.g., Brie and Saiki, 1996). Other late-arriving modes in the dipole waveform, such as fluid wave and Stoneley modes, are eliminated by selecting a variable processing time window length of 9,999–11,499 ms and a fixed slowness range from 280 to 1080 ms/ft. Bandpass filtering and time windowing are performed to extract the flexural mode of the dipole waveforms from both logging passes. The *S*-wave slowness is determined automatically by picking the arrival time of the flexural wave from the filtered data at 16 receivers (orthogonal dipole receivers at the eight stations). In general, pass 2 data have higher signal-to-noise due to the use of the lower-frequency dipole source. The signal-to-noise energy ratio is sufficiently high to obtain results from 226 to 350 mbsf for pass 1 and over the entire interval for pass 2.

Below 350 mbsf, however, only receiver stations 1–5 were selected in the pass 2 data and 32 points/cycle were used for phase picking. The flexural mode is so weak in this interval that the farthest three stations along the tool array have insufficient signal-to-noise ratios for picking and were eliminated before processing. The weak flexural mode energy in this interval also limited the processing to ~80% of the first period and required that a higher sampling density be used. Testing indicates that using only five stations and the shorter sampling period agrees well with the result of normal processing in other intervals where the flexural wave signal is strong.

RESULTS AND COMPARISONS

The processed *P*-wave slowness logs from both passes are shown in Figure F5. Only those intervals where reliable *P*-wave slowness is computed are shown, as well as the preliminary shipboard *P*-wave logs from both passes for comparison. Both passes are generally of high quality over the entire interval. The trends of the shipboard and reprocessed logs agree, and variations in the shipboard log above 180 mbsf are eliminated. Enlarged hole size and switching between the high-energy fluid and *P*-wave modes affected the shipboard log in this interval. Note that below 260 mbsf, the reprocessed log for pass 1, but not pass 2, is 10–15 ms/ft slower than the shipboard log.

F4. Model of dipole pole excitation, p. 11.

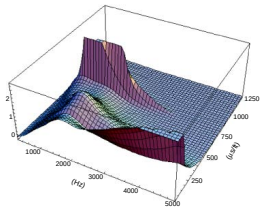

F5. Comparison of raw and reprocessed *P*-wave logs, p. 12.

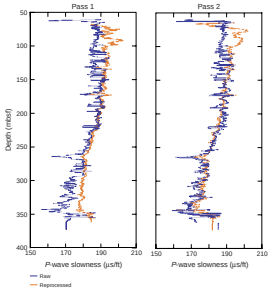

The processed *S*-wave slowness logs from both passes are shown in Figure F6. Only those intervals where reliable *S*-wave slowness is computed are shown, as well as the preliminary shipboard logs from both passes for comparison. The *S*-wave logs are of high quality over the interval from 226 to 350 mbsf for pass 1 and from 65 to 360 mbsf for pass 2. Above 226 mbsf, pass 1 data have poor signal-to-noise ratio and reliable values could not be picked. In the overlapping interval, reprocessed *S*-wave logs from both passes generally follow the trends of the shipboard logs. Above 226 mbsf, the reprocessed data from pass 2 measure *S*-wave slowness values up to 1100 ms/ft. This is 50–150 ms/ft higher than the shipboard values over this interval. The pass 2 reprocessed log confirms the presence of the velocity inversion below 350 mbsf, and *S*-wave slowness values reach 1000 ms/ft (V_S = 305 m/s) at their maximum. Use of the low-frequency dipole source enables sufficient signal-to-noise ratio in these intervals to accurately extract the *S*-wave velocity.

The processed *P*- and *S*-wave logs from pass 1 and 2 are compared in Figure F7. The trend and vertical resolution of both *P*-wave passes agree closely from 65 to 360 mbsf. Core plug measurements (vertical orientation) are systematically 8–12 ms/ft higher than both passes. The offset between the core and log measurement can be attributed to the higher porosity (lower velocity) of core measurements made under ambient surface conditions (e.g., Goldberg et al., 1987). In this case, porosity rebound of the core measurements varies from 1.5% to 6.5%, with the largest difference occurring at ~226 mbsf, perhaps related to lithologic changes at this depth.

The *P*-wave slowness values from pass 1 are systematically 2–4 ms/ft higher than those from pass 2. The peak *P*-wave amplitude and frequency also differ between the two passes. Peak frequency is ~1.5 kHz (20%) higher, and amplitudes are three times higher in pass 1 than pass 2. Testing indicates that these differences are not due to filtering prior to processing. The monopole source was nominally operating at the same frequency between passes, and it is unlikely that use of the DSI low-frequency dipole source during pass 2 could affect the monopole transmitter frequency, according to Schlumberger. They have completely different circuits, and line voltage fluctuations will not change the frequency of the source. Since hole conditions did not change, a possible explanation of these offsets is a change in centralization of the tool between passes. Tool eccentralization will cause drastic reduction in amplitude of the monopole signal (e.g., Goldberg et al., 1984), and this reduction could introduce frequency and phase-picking shifts. Further studies may be undertaken to extract the *P*-wave component of the dipole signal (a low-amplitude precursor to the flexural mode) for comparison. This mode propagates differently in the borehole and could help to explain the observed offsets between the two passes using the monopole source.

The *S*-wave logs agree well over the interval 226–350 mbsf where the two intervals overlap. The trend and vertical resolution of both passes reproduce closely. As noted above, pass 1 dipole data have poor signal-to-noise ratio in low-velocity intervals. Pass 1 *S*-wave slowness values are not reliable above 226 mbsf or below 350 mbsf. The low-frequency dipole source used for pass 2 gives reliable slowness values over the entire logged interval and confirms the velocity inversion below 350 mbsf. The *S*-wave slowness values for pass 2 above 226 mbsf are significantly greater than the shipboard results. Use of the unprocessed *S*-

F6. Comparison of raw and reprocessed *S*-wave logs, p. 13.

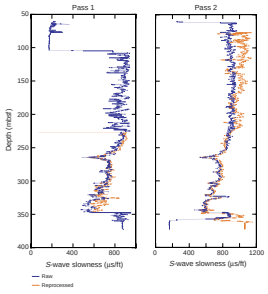

F7. Comparison of reprocessed *P*- and *S*-wave logs, p. 14.

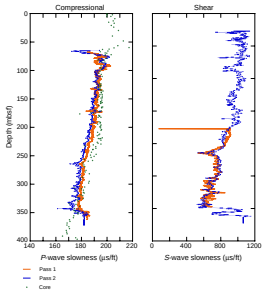

wave velocities may introduce errors of 20% or more in these shallow sediments.

Figure F8 shows crossplots of *P*- vs. *S*-wave slowness from shipboard results and from the current reprocessing. The difference in the range of *P*- and *S*-wave slowness is considerable, but both data sets have relatively linear relationships with correlation coefficients >0.80. Data points above *P*-wave values of 180 ms/ft have significantly greater scatter. Linear regression of the processed results yield the relationship

$$DTc = 150 + 0.0389\ DTs\ (R = 0.83).$$

A similar regression of the shipboard data yields

$$DTc = 139 + 0.0587\ DTs\ (R = 0.86),$$

which has ~33% greater slope than for the reprocessed logs. Core measurements of *P*- and *S*-wave velocity should be compared to the reprocessed logs to further confirm the improved accuracy and reliability of these results.

F8. Crossplots of *P*- vs. *S*-wave logs, p. 15.

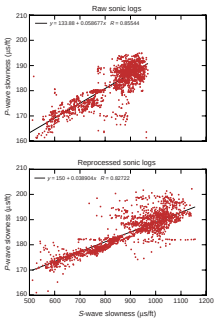

SUMMARY

The reprocessing of the DSI wireline logs using a phase-picking technique allows for extraction of improved *P*-wave and *S*-wave logs from these data. Artifacts in the *P*-wave log due to mode switching and in the *S*-wave log due to flexural wave resonance were removed. Dispersion corrections were not required in these low-velocity sediments. The *P*-wave log shows systematically higher velocity than from core measurements due to porosity rebound. *S*-wave log velocities as low as 280 m/s were measured using the DSI tool in the interval above 100 mbsf and below 350 mbsf at Site 1173. The reprocessed logs are available directly via the ODP online log database at **www.ldeo.columbia.edu/BRG/ODP/DATABASE/index.html.** These data should be used in place of the shipboard logs for future research studies.

ACKNOWLEDGMENTS

This research used data provided by the Ocean Drilling Program (ODP). The ODP is sponsored by the U.S. National Science Foundation (NSF) and participating countries under management of Joint Oceanographic Institutions (JOI), Inc. Harold Tobin (LDEO Logging Scientist) supervised shipboard data acquisition and quality control during ODP Leg 190. Trevor Williams and Cristina Broglia (LDEO Borehole Research) prepared the DSI data for postcruise work. Jeff Williams and Marek Kozak (SuperSonic Geophysical) provided software to process these data and ran the models shown in Figure F4. Kazuko Nagao assisted with figure preparation for the manuscript. The efforts of these collaborators and the crew and staff of the *JOIDES Resolution* during Leg 190 are greatly appreciated. The U.S. Science Support Program provided funding for this research.

REFERENCES

Brie, A., and Saiki, Y., 1996. Practical dipole sonic dispersion correction. *Trans. Soc. Expl. Geophys.,* 178–181.

Goldberg, D., 1990. Test performance of the Ocean Drilling Program wireline heave motion compensator. *Sci. Drill.,* 1:206–209.

————, 1997. The role of downhole measurements in marine geology and geophysics. *Rev. Geophys.,* 35:315–342.

Goldberg, D., Kan, T.K., and Castagna, J.P., 1984. Attenuation measurements from sonic log waveforms. *Trans. Soc. Prof. Well-Log Analysts,* 26:NN.

Goldberg, D., Wilkens, R.H., and Moos, D., 1987. Seismic modeling of diagenetic effects in Cenozoic marine sediments at Deep Sea Drilling Project Sites 612 and 613. *In* Poag, C.W., Watts, A.B., et al., *Init. Repts. DSDP,* 95: Washington (U.S. Govt. Printing Office), 589–599.

Kimball, C.V., and Marzetta, T.L., 1984. Semblance processing of borehole acoustic array data. *Geophysics,* 49:274–281.

Kozak, M., Boonen, P., and Siefert, D., 2001. Phase velocity processing for acoustic logging-while-drilling full waveform data. *Trans. Soc. Prof. Well-Log Analysts*, 42:PP.

Moore, G.F., Taira, A., Klaus, A., and Leg 190 Scientific Party, 2001. New insights into deformation and fluid flow processes in the Nankai Trough accretionary prism: Results of Ocean Drilling Program Leg 190. *Geochem. Geophys. Geosyst.,* 2:10.129/2001GC000166.

Paillet, F.L., and White, J.E., 1982. Acoustic modes of propagation in the borehole and their relationship to rock properties. *Geophysics,* 47:1215–1228.

Shipboard Scientific Party, 2000. Leg 190 Preliminary Report. *ODP Prelim. Rpt.,* 90 [Online]. Available from World Wide Web: <http://www-odp.tamu.edu/publications/prelim/190_prel/190PREL.PDF>.

————, 2001a. Explanatory notes. *In* Moore, G.F., Taira, A., Klaus, A., et al., *Proc. ODP, Init. Repts.,* 190, 1–51 [CD-ROM]. Available from: Ocean Drilling Program, Texas A&M University, College Station TX 77845-9547, USA.

————, 2001b. Leg 190 summary. *In* Moore, G.F., Taira, A., Klaus, A., et al., *Proc. ODP, Init. Repts.,* 190, 1–87 [CD-ROM]. Available from: Ocean Drilling Program, Texas A&M University, College Station TX 77845-9547, USA.

————, 2001c. Leg 196 Preliminary Report. *ODP Prelim. Rpt.,* 96 [Online]. Available from World Wide Web: <http://www-odp.tamu.edu/publications/prelim/196_prel/196PREL.PDF>.

————, 2001d. Site 1173. *In* Moore, G.F., Taira, A., Klaus, A., et al., *Proc. ODP, Init. Repts.,* 190, 1–147 [CD-ROM]. Available from: Ocean Drilling Program, Texas A&M University, College Station TX 77845-9547, USA.

Winbow, G.A, 1985. Compressional and shear arrivals in multipole logs. *Geophys.,* 50:1119–1126.

Figure F1. Schematic of the Schlumberger Dipole Shear Imager (DSI) tool.

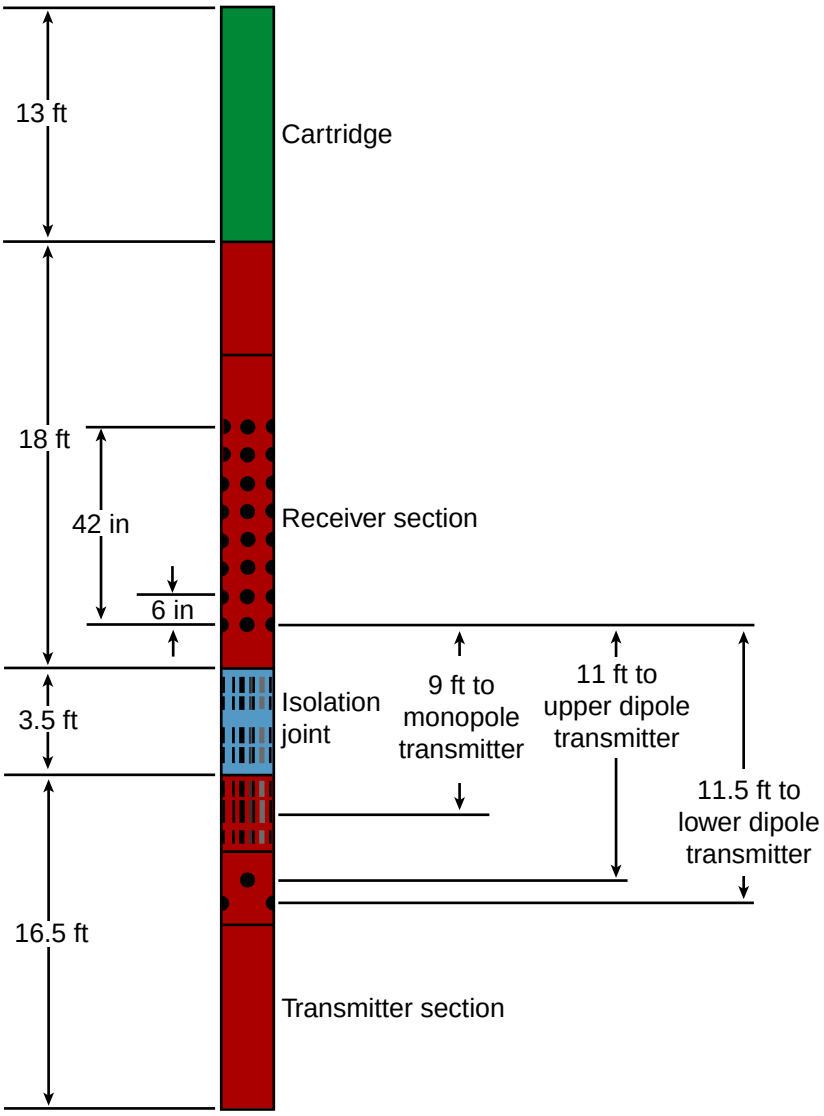

Figure F2. Caliper logs from two passes with the DSI tool in Hole 1173A. Two curves represent orthogonal diameters of the borehole as a function of depth. The hole was drilled with a 9.875-inch bit. The borehole is enlarged above 226 mbsf, but its shape does not change significantly between pass 1 and pass 2.

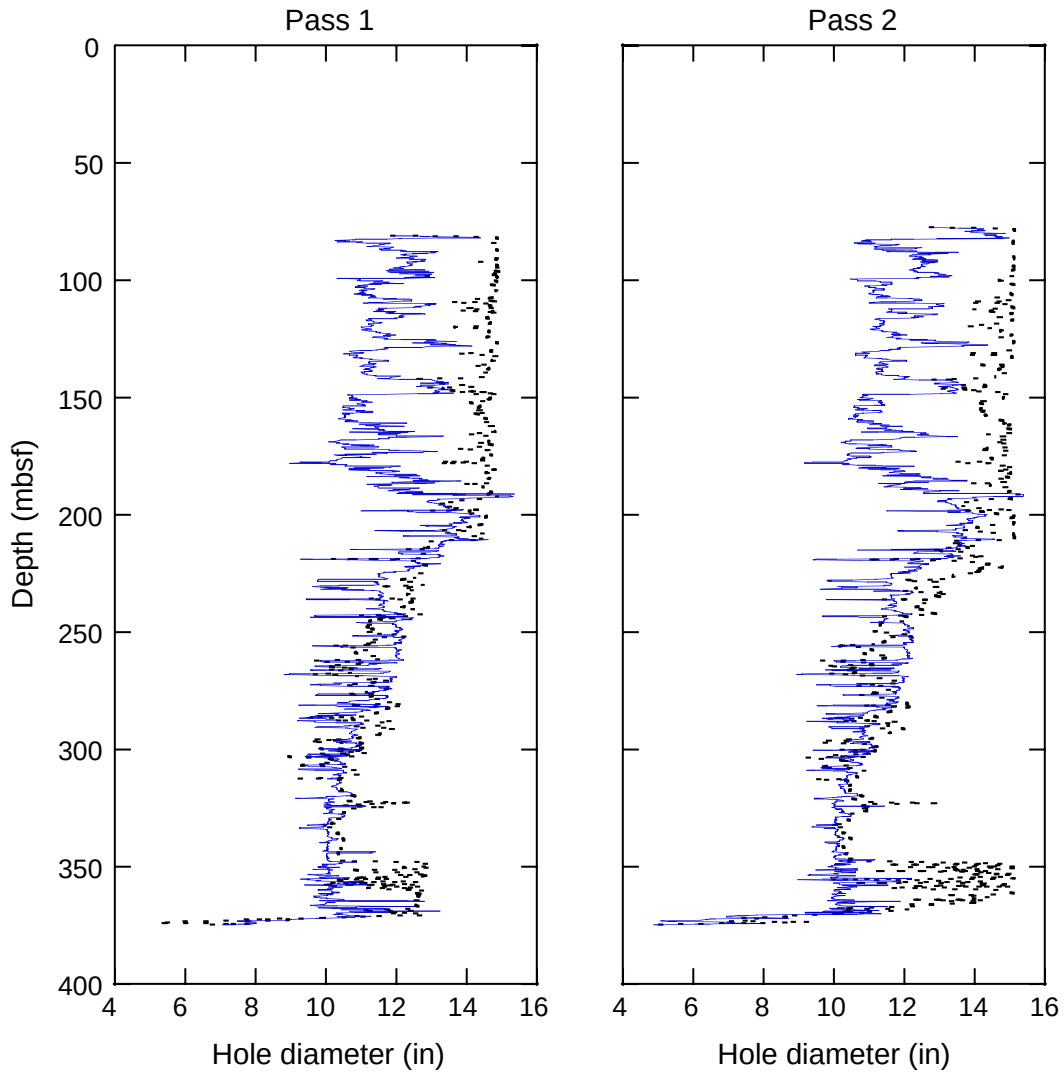

Figure F3. Time and frequency displays of wireline DSI data (pass 1) from ~250 to 350 mbsf in Hole 1173A. Red = high and blue = low acoustic energy over the 0- to 20-kHz frequency band. Much of the observed monopole energy above 10 kHz is not useful for *P*-wave processing. The dipole energy occurs below 1.5 kHz. Both data sets require filtering and processing to extract reliable velocity information.

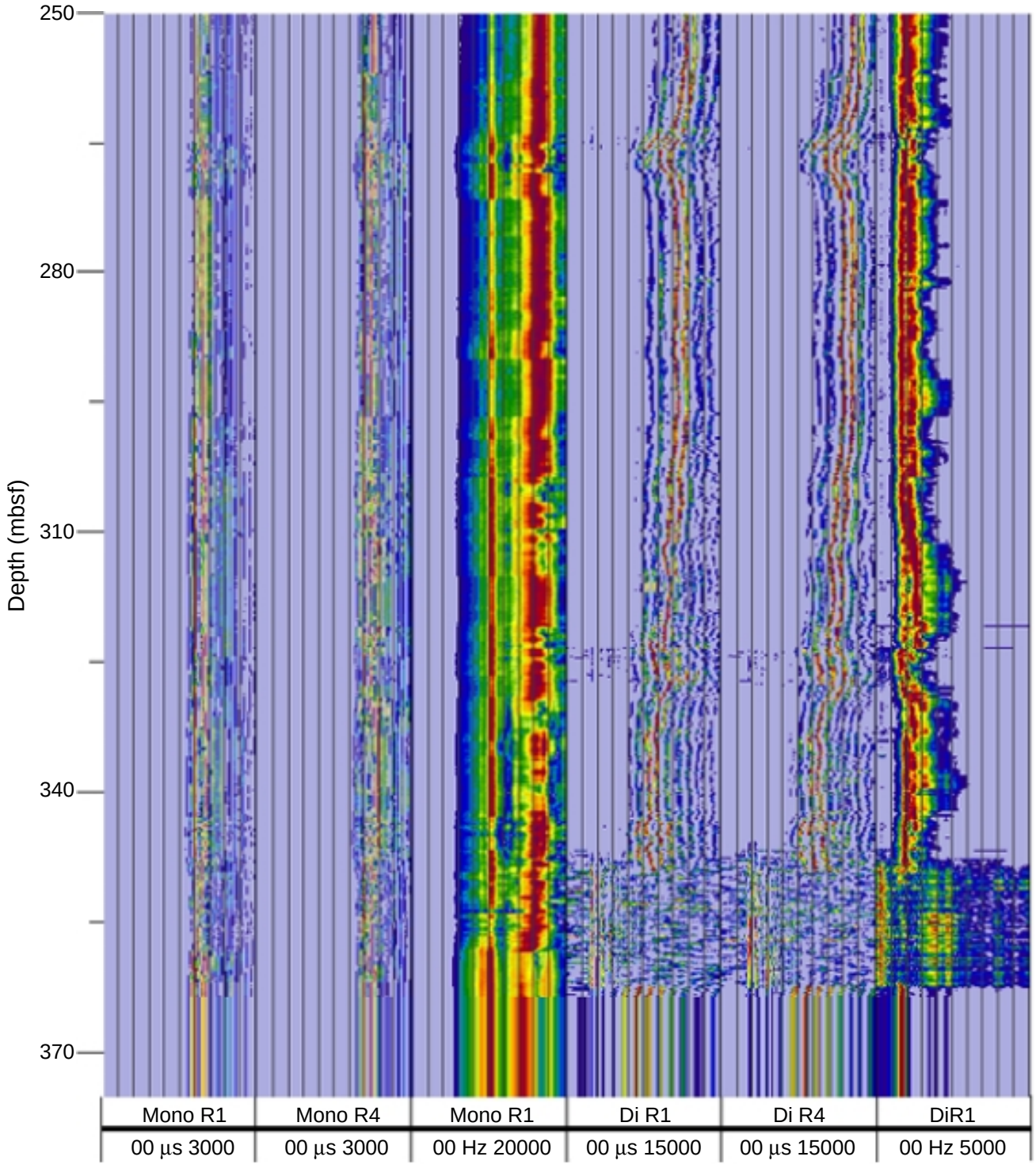

Figure F4. Model of dipole pole excitation (relative amplitude) as a function of frequency and slowness. The major resonance peak on this surface occurs near 780 ms/ft and at ~1000 Hz. Modeling also indicates that the dipole mode is nondispersive below 500 Hz.

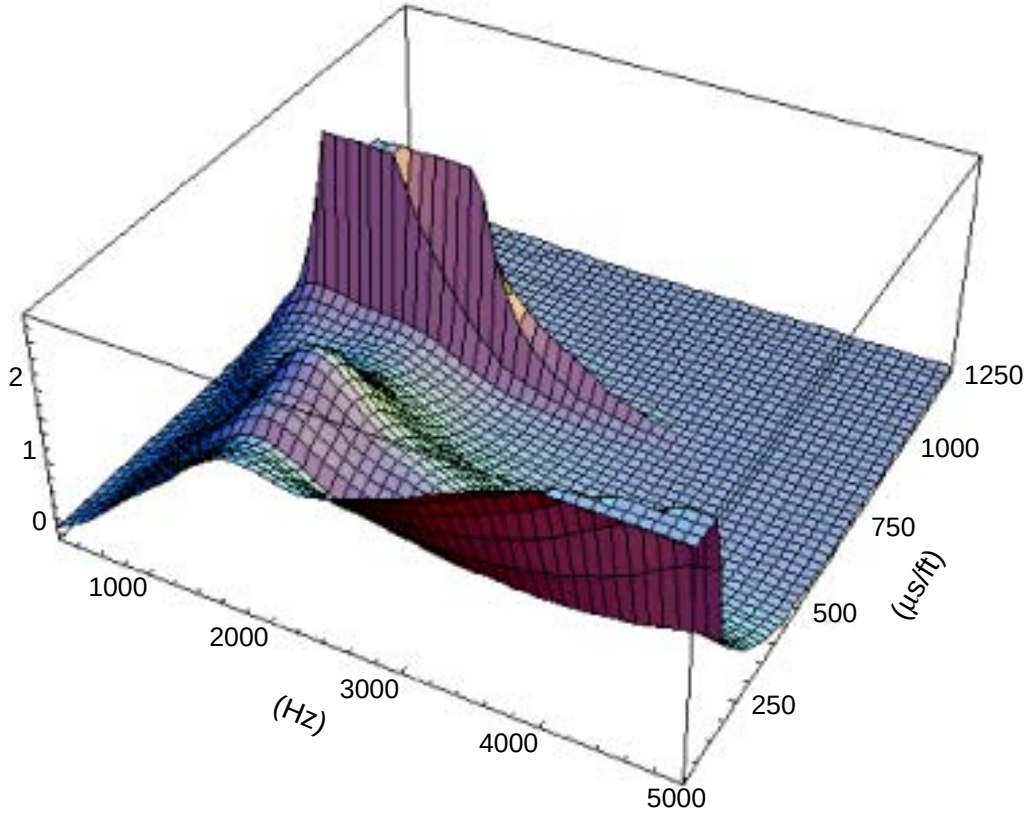

Figure F5. Comparison of shipboard and reprocessed *P*-wave slowness logs as function of depth from pass 1 and pass 2 in Hole 1173A. Reprocessed curves show less variation above 226 mbsf (enlarged hole) where mode switching significantly affected the shipboard logs. The velocity inversion below 350 mbsf is present in both shipboard and reprocessed logs.

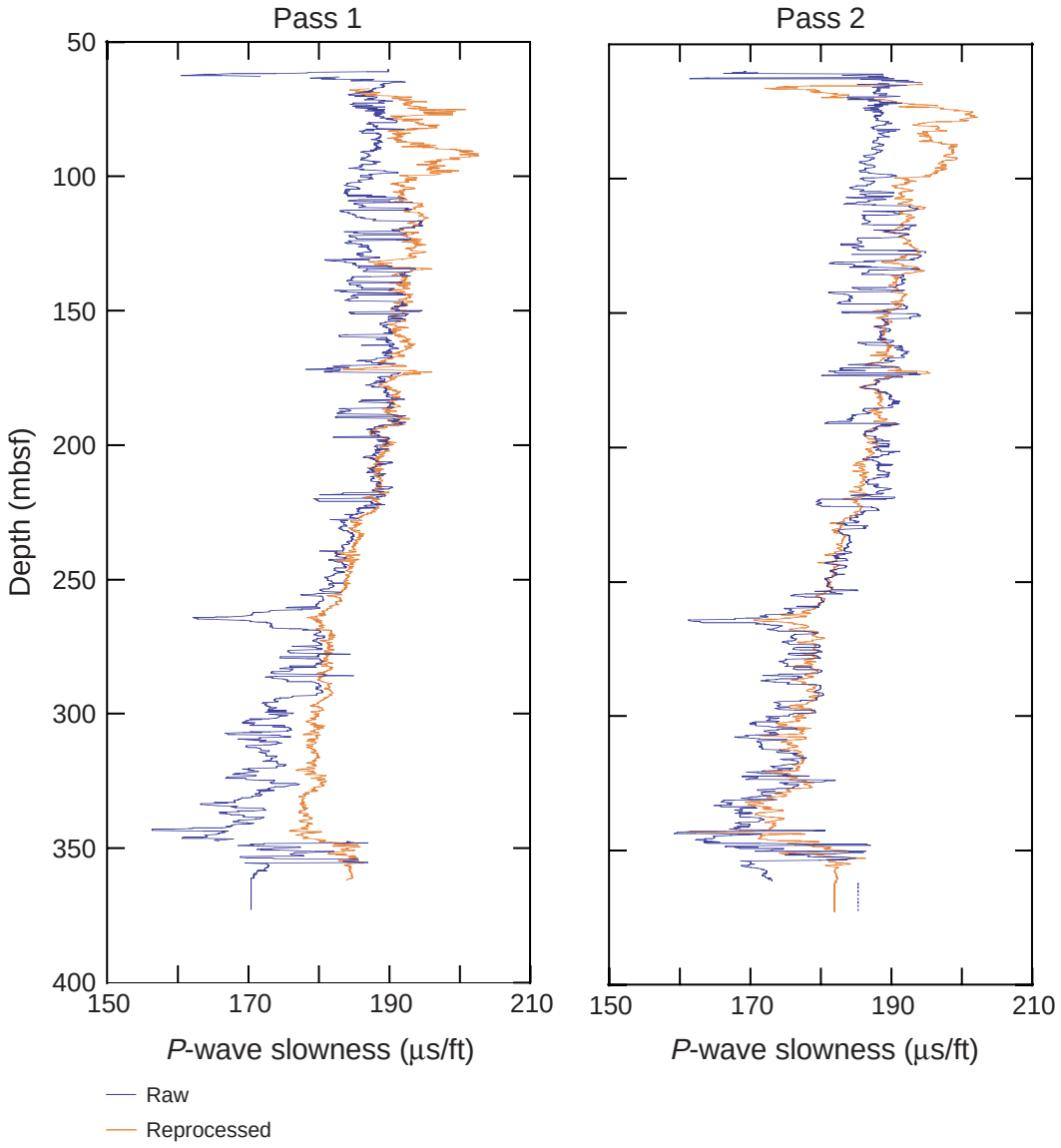

Figure F6. Comparison of shipboard and reprocessed *S*-wave slowness logs as function of depth from pass 1 and pass 2 in Hole 1173A. Pass 2 data has higher signal-to-noise ratio due to the use of the low-frequency DSI source, allowing reliable *S*-wave slowness to be extracted over the entire logged interval. Pass 1 data are used to extract reliable results from 226 to 350 mbsf. The velocity inversion below 350 mbsf is confirmed in the reprocessed pass 2 log.

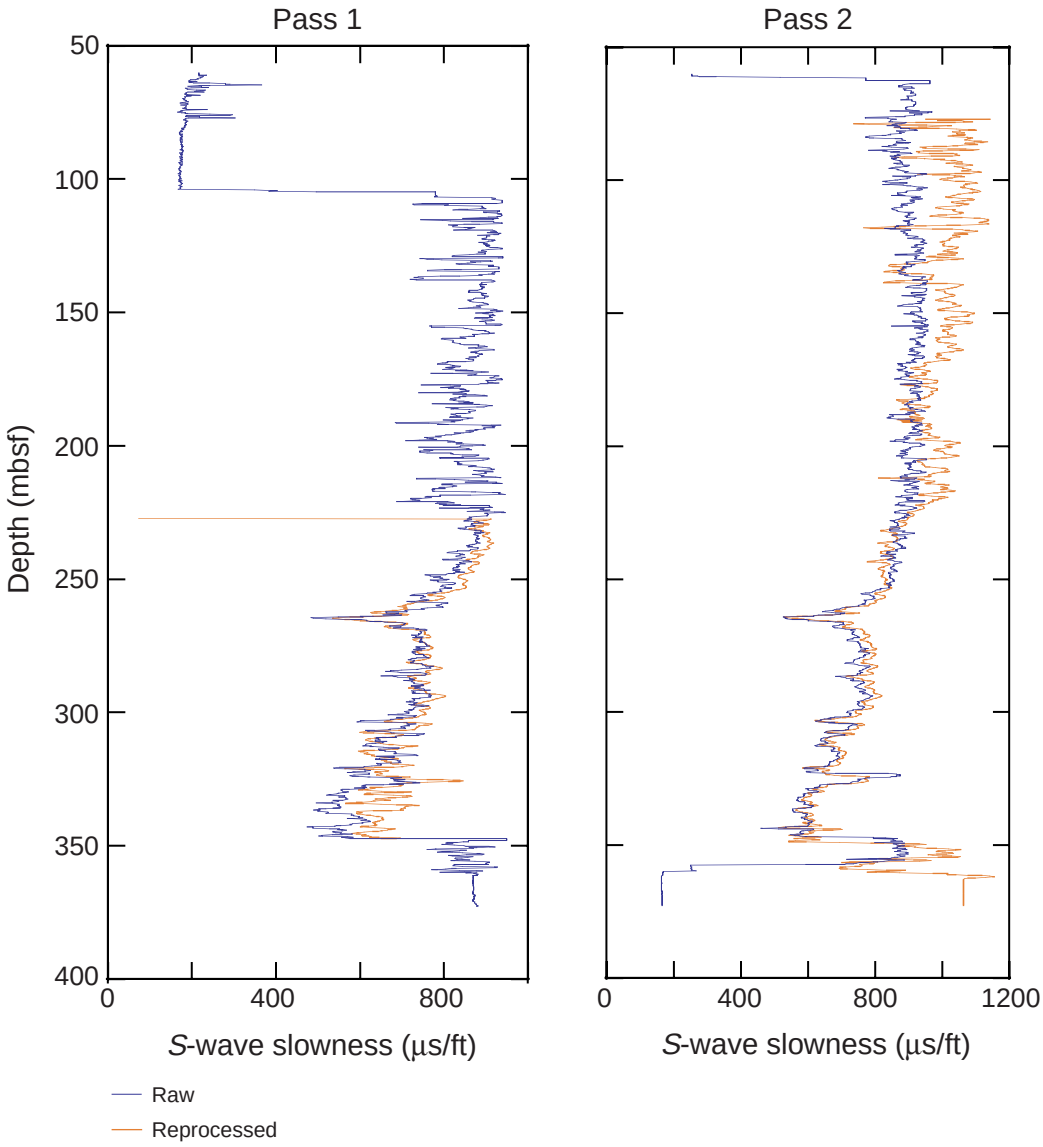

Figure F7. Comparison of reprocessed *P*- and *S*-wave slowness logs as a function of depth from pass 1 and pass 2. Core *P*-wave values are also shown. The trends of the two reprocessed *P*-wave passes and core data generally agree, but pass 2 is systematically 2–4 µs/ft faster than pass 1 and 8–12 µs/ft faster than the core values. The trends of the two reprocessed *S*-wave curves agree well over the overlapping interval.

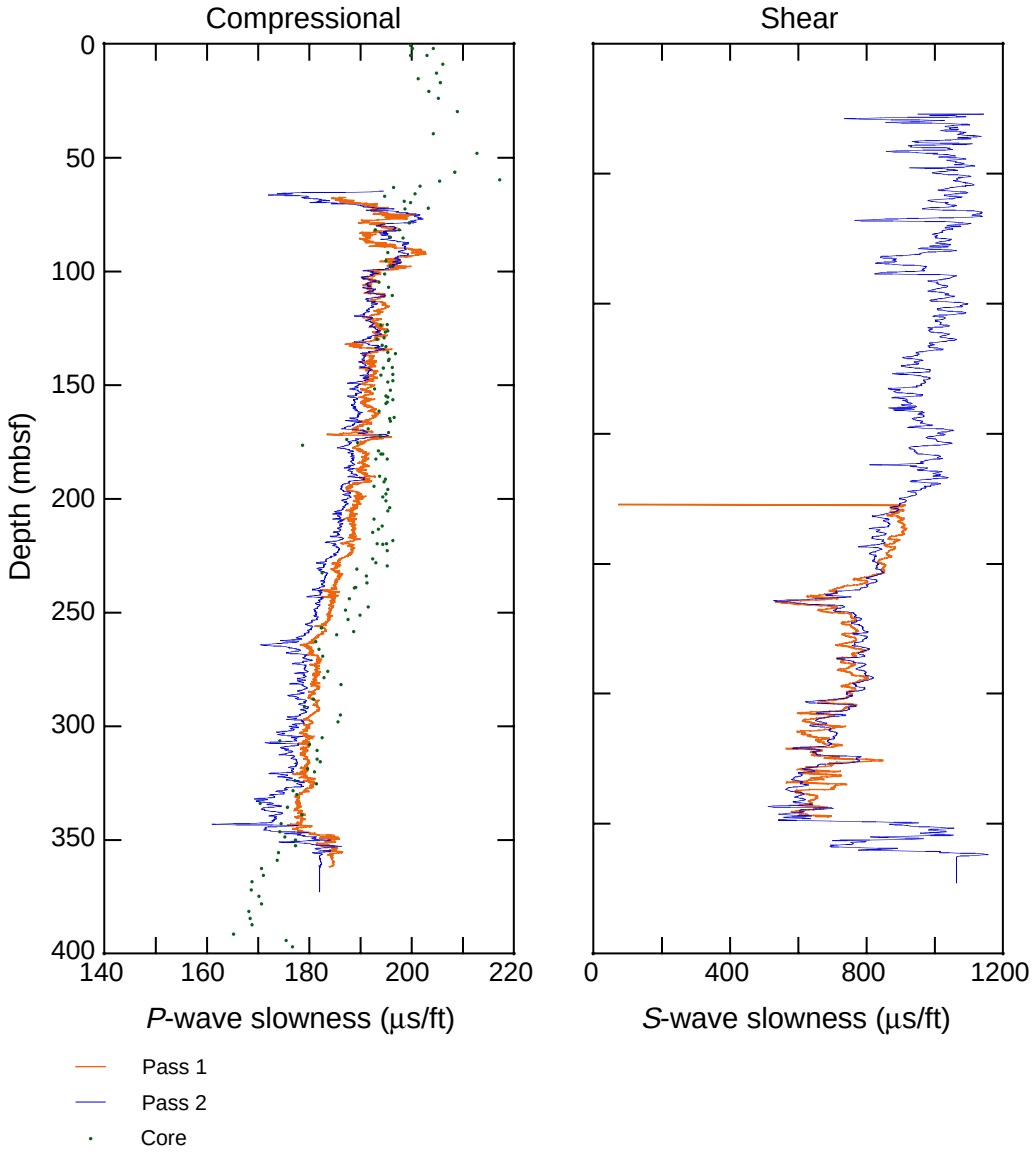

Figure F8. Crossplots of *P*- vs. *S*-wave slowness from both shipboard and reprocessed data. Linear regression of the reprocessed data yield the relationship DTc = 150 + 0.0389 DTs (R = 0.83). The average slope of this regression is 33% lower than that from shipboard results.